# INVERSE TEST BASED ESTIMATION OF EQUIVALENT ACOUSTIC EXCITATION BASED ON AIRCRAFT CABIN RESPONSE MEASUREMENTS

Authors: Prof. Dr. Benedikt Plaumann, Prof. Dr. Thomas Kletschkowski, Mr. Ashish Chodvadiya, Mr. Eugen Hein; Hamburg University of Applied Sciences

## Introduction

This contribution describes the concept and its implementation of creating an equivalent acoustic broadband random excitation outside a aircraft fuselage section that creates the same response spectrum inside the passenger cabin as in a real flight, as depicted in Figure 1. For this, reference measurements in real flights with similar A320 (CEO - Classic Engine Option) have been recorded in the same location of the fuselage as in the test setup. The measured real flight cabin acoustic spectrums are therefore used as response reference target spectrums which are to be replicated by a suitable excitation outside the fuselage in the echoic climate chamber.

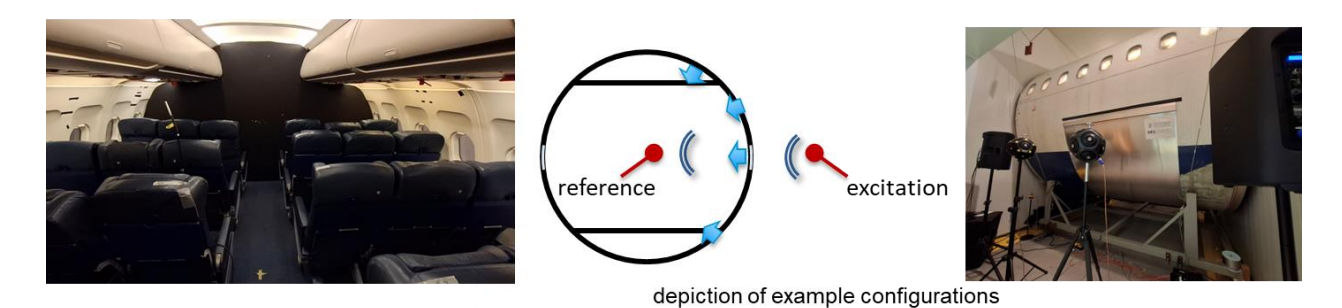


Figure 1: Concept of creating an equivalent response spectrum in the cabin as in real flights by an adapted acoustic excitation in the acoustic climate chamber outside of the fuselage section.

Later an outlook is given how transfer paths from outside to inside through air and structure can be measured with real hardware in the loop. The implementation is based on an Airbus A320CEO fuselage section (aft of the center wing box). The fuselage section is closed with acoustically absorbing bulkheads with very low transmission at both ends. The fuselage section is situated in an acoustic climate chamber that can control temperature on the outside and temperature as well as humidity inside the cabin. The whole setup is situated at the lab of Cabin and Cabin Systems of the HAW Hamburg at their venue in the Hamburg Center for Aviation Training (HCAT). The measurement and excitation equipment are provided mostly by the Research and Transfer Center for Technical Acoustics of the HAW Hamburg. The presentation at SAVE was funded by the Research and Transfer Center Future Air Mobility by the Hamburg University of Applied Sciences (HAW Hamburg).

# STATE OF THE ART

Continuously improving safety and passenger comfort while ensuring ecological and economic efficiency is a major challenge for the modern aviation industry. An important focus is the acoustic optimization of aircraft cabins, as an appropriate interior noise level is crucial for the comfort and communication of passengers and crew. Current noise reduction measures often lead to a significant increase in weight, which increases fuel consumption and reduces aircraft efficiency. Additional weights of several 100kg to a few tons per aircraft show the potential for significant efficiency improvements and CO<sub>2</sub> reductions. Due to the high cost and complexity of real flight tests in early stages of development, ground tests simulating acoustic fields during flight with loudspeaker arrays in laboratory are

carried out instead. These tests allow the evaluation of noise reduction measures under controlled conditions but usually use a simple broadband white noise that cannot replicate the specific acoustic characteristics of real flight conditions, limiting the accuracy of noise reduction assessments [1].

In studies like [2] and [3], white noise was used in the climate chamber of the HCAT, where A320 segment located, to evaluate the sound transmission paths in the cabin. Three dodecahedral loudspeakers (800 W each) were used in these very first test setups, resulting in a total sound pressure level of 67 dB(A) in the cabin. However, the in-flight measurements on an Airbus A321 narrow-body aircraft presented in the study [4] showed total sound pressure levels of 60-65 dB(A) before take-off, 80-85 dB(A) during flight and 75-80 dB(A) on landing. In another study [5], wide-body aircrafts, including the Airbus A330 and the Boeing B777, were analyzed in various phases of flight. The average sound pressure levels measured were 68.7 dB(A) during taxiing, 75.7 dB(A) during take-off, 71.3 dB(A) during cruising, and 72.9 dB(A) during landing of the A330. These results show that the noise levels in the cabin vary considerably during the different phases of flight. The results of the study, based on Airbus A320 flight tests conducted as part of the German national project SIMKAB (LuFo IV) shows that the cabin noise is also depends on different flight speeds, altitudes, and operational conditions of the engines and air conditioning system [6].

The sound pressure levels inside the aircraft cabin vary not only depending on the flight condition but also on the passenger's seating position. The frequency spectrum of cabin noise can be simplified as broadband noise, with the maximum frequency and frequency rise varying depending on the position in the cabin. In the forward area, the spectrum reaches a high-frequency maximum peak between 1 kHz and 4 kHz. In the middle cabin, the maximum is between 600 Hz and 800 Hz, while in the rear area, a low-frequency spectrum with peak levels between 250 Hz and 500 Hz predominate [7]. Therefore, white noise cannot adequately reflect the complex noise environment in the cabin. To change this, excitation profiles need to be customized to specific flight phases to achieve realistic noise conditions in test setups, allowing for a more accurate assessment of cabin noise.

Sound field control (SFC) technology enables the active control of audio transmission in an acoustic environment. It comprises three research areas: Sound field reproduction, personal audio systems and active noise control. Sound field reproduction uses loudspeaker arrays to replicate a sound field in a target region; personal audio systems extend sound field reproduction to multiple regions so that different listeners in a shared space can hear personalized audio signals; and active noise control aims to cancel out the original sound field in the target area by creating a secondary sound field[8]. This study focusses on sound field reproduction, as it allows a precise reproduction of a defined sound field and seems particularly suitable for reproducing cabin acoustics.

A sound field reproduction system reproduces the desired sound field over a target region with the help of loudspeaker arrays. The three main methods are wave field synthesis (WFS), which uses Huygens' principle to replicate sound fields but faces challenges like aliasing and practical speaker limitations; Higher-Order ambisonics (HOA), which employs spherical harmonics for precise reproduction but requires complex speaker setups; and the pressure matching (PM) method, which simplifies implementation by focusing on sound pressure at specific control points. Due to its practicality, the PM method is emphasized in this work [8].

Liu et al. [9] developed a sound field reproduction (SFR) system within an aircraft mock-up to evaluate active noise cancelling (ANC) devices under realistic conditions. The system uses a multi-channel least-mean-square (LMS) algorithm with feedback control and Tikhonov regularization, which achieves high accuracy by minimizing reproduction errors and eliminating instabilities due to ill-conditioned inputs. The benefits of this study include accurate reproduction of complex acoustic fields and realistic test conditions for ANC devices, with errors reduced to less than 3 dB. However, the practical challenges are associated with the use of a large number of 32 microphones and 27 loudspeakers, which complicates setup and drives up costs, as well as the challenges of reproducing sound fields affected by reflections and standing waves.

Between 2012 and 2016, Gauthier et al. ([10],[11],[12]) developed a sound field reproduction (SFR) algorithm to replicate realistic aircraft cabin acoustics using a Bombardier cabin mock-up. The key innovations involved multichannel least squares control with Tikhonov regularization, frequency-specific parameter tuning and acoustic imaging. These advances significantly improved reproduction accuracy, especially in the difficult low-frequency range, and enabled accurate simulation of real aircraft sounds for acoustic analyses and comfort studies. However,

limitations included the practical challenges of using large setups with 41 actuators and 80 microphones, as well as the complexity and computational cost of system modelling and transfer function measurements.

Since the methods mentioned above are very complex, an equivalent acoustic excitation was generated in this study using measurement data of the in-flight cabin as a reference. The excitation signal was generated by adjusting the white noise parameters with Audacity software to simulate the acoustic environment of flight. This excitation was generated by 10 loudspeakers with different specifications to simulate realistic sound fields.

The main objective of the test setup was to investigate the global sound transmission paths from the outside to the inside cabin environment, focusing on the non-linearity of these transmission paths. The acoustic window method was used to analyze the sound transmission paths, where each structural panel was treated as an acoustic window. See also [13] for more information. The sound intensity was measured for the defined panel, which was assumed to be in the anechoic chamber and to have the same incidence area and transmission area. The sound transmission loss (STL) was then calculated using formulae 1 according to [13] as in [14].

$$STL = L_p - 6dB - L_w \tag{1}$$

where STL is sound transmission loss,  $L_p$  is sound pressure in diffuse field (anechoic chamber) in dB,  $L_w$  is sound intensity of the defined panel in dB.

In addition, a detailed analysis of airborne and structure-borne noise contributions within the same transmission path was carried out in this paper as an outlook to this study. The differentiation of these contributions was considered crucial in determining the predominant transmission mechanism. In cases where structure-borne noise was identified as the main contributor, reduction techniques were suggested, such as the use of vibration isolators between the external and internal structure [15]. This approach was developed to attenuate vibrations and reduce sound transmission.

An example for structureborne sound reduction analysis to be performed with the setup is shown in [15] for individually designed, 3d-printed Thermoplastic PolyUrethan (TPU) elastomers in the structural sound transmission.

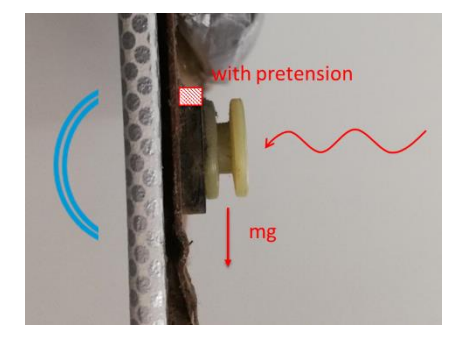


Figure 2: Static loads (pretension and weight) and dynamic loads (sideways acoustic excitation) acting on a sidewall panel fixation with already implemented reduction method of elastomer block (black) from A320CEO cabin.

Figure 2 shows that it is necessary to design improved isolators for, in this case a classic A320CEO lower sidewall panel fixations according to the following design requirements with varying parametric values:

- Maximum quasi-static loads, i.e. from EASA CS25 [16] emergency landing conditions accelerations, design parameter: strength
- Minimum stiffness in a limited acoustic deflection range, also considering static gravitation loads (1g) from mass to carry.

Depending on the needed pretention to support the panels weight and kept the operational deflection within the small yielding range before the isolator goes into block for maximum strength requirements, these requirements vary for different weights to be supported with pretention and maximum stress loads in each degree of freedom. With a setup as presented, quickly designed new isolators can be tested in-situ under realistic excitation and transmitted powers, even considering non-linear behavior. This is very important because isolators designed as presented in [15] show a

highly non-linear behavior towards excitation amplitude because they go into block when the excitation exceeds the yielding acoustic range and enters the maximum strength range. A well to the requirements designed isolator would be rather yielding under low deflections of acoustic excitation and then go into block with maximum stiffness and stress i.e., under emergency landing loads. Other non-linearities of deformation and material properties may also occur. Therefore, it is very important to work with realistic excitation levels.

## **METHODS**

The measured acoustic audio spectrums are derived from a data set taken on four different flights with A320 CEO and derivatives while seated in the same fuselage section as implemented in the lab environment, see Figure 3. The measurements have been taken with a clear focus to derive reference material from different flight and operation situations of the aircraft. The data set include different operation and flight phases of the four aircraft like taxi, take-off acceleration, initial climb, climb cruise, very low engine RPM cruise ("sailing"), initial and final descend, approach, touch-down and braking as well as "engine off, Air-Con on", "engine starting" conditions. Also, a few measurements are taking with significant passenger background talk in the cabin, but the absolute majority is without. The cruise speed and altitude given are derived either from information on the Inflight Entertainment or external flight tracker data.

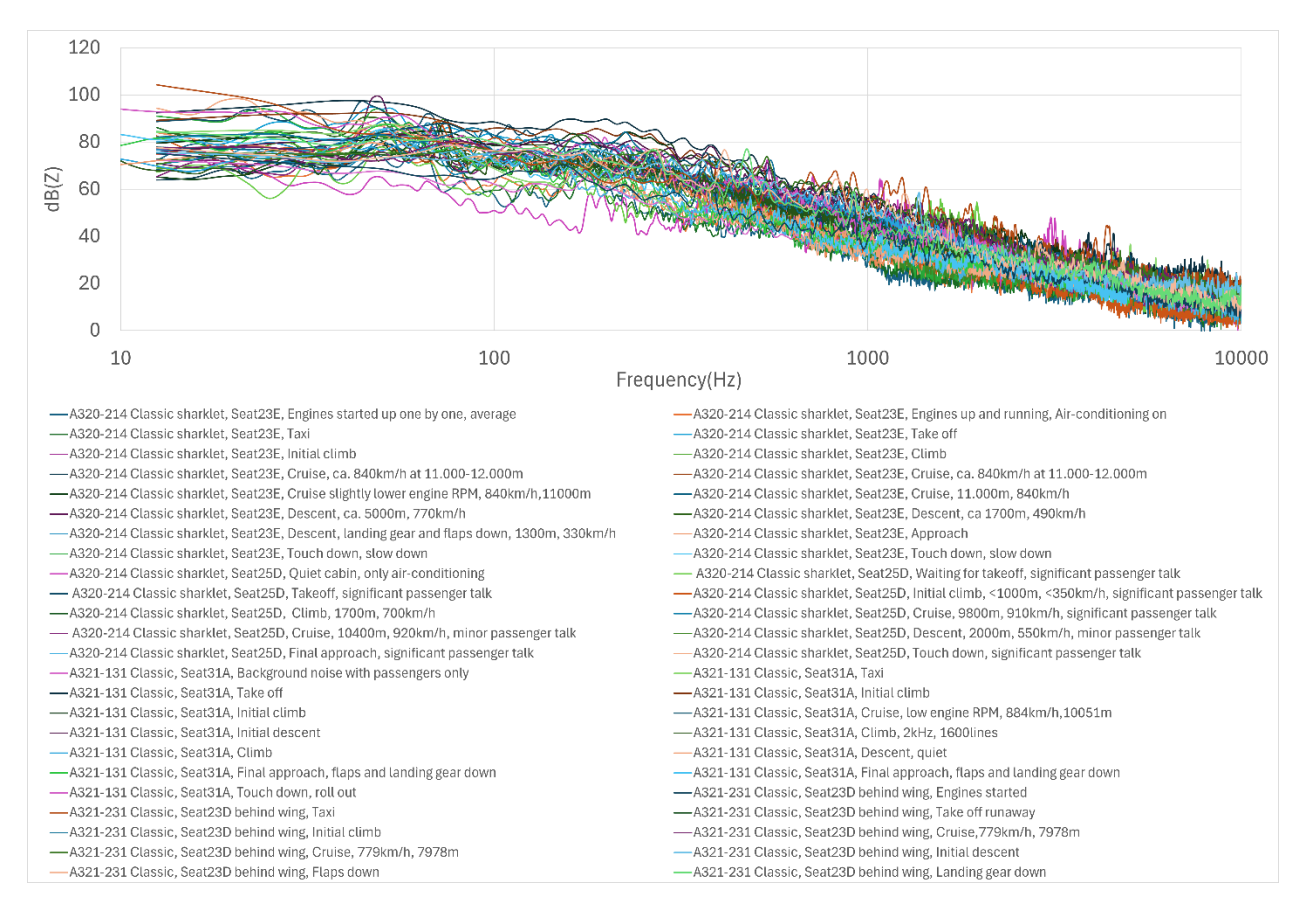


Figure 3: Overview of spectrums of the general data sets provided. For the later replication of a cruise phase only some measurements where considered.

Even though the data set enables a possible statistical analysis like in "design of experiments" [17] to quantify the different influence factors, this contribution only looks at the measurements in a late and rather quiet cruise phase at around 10-12km flight level (and two at 8km) without significant passenger background noise and low noise levels from air conditioning as shown in Figure 4.

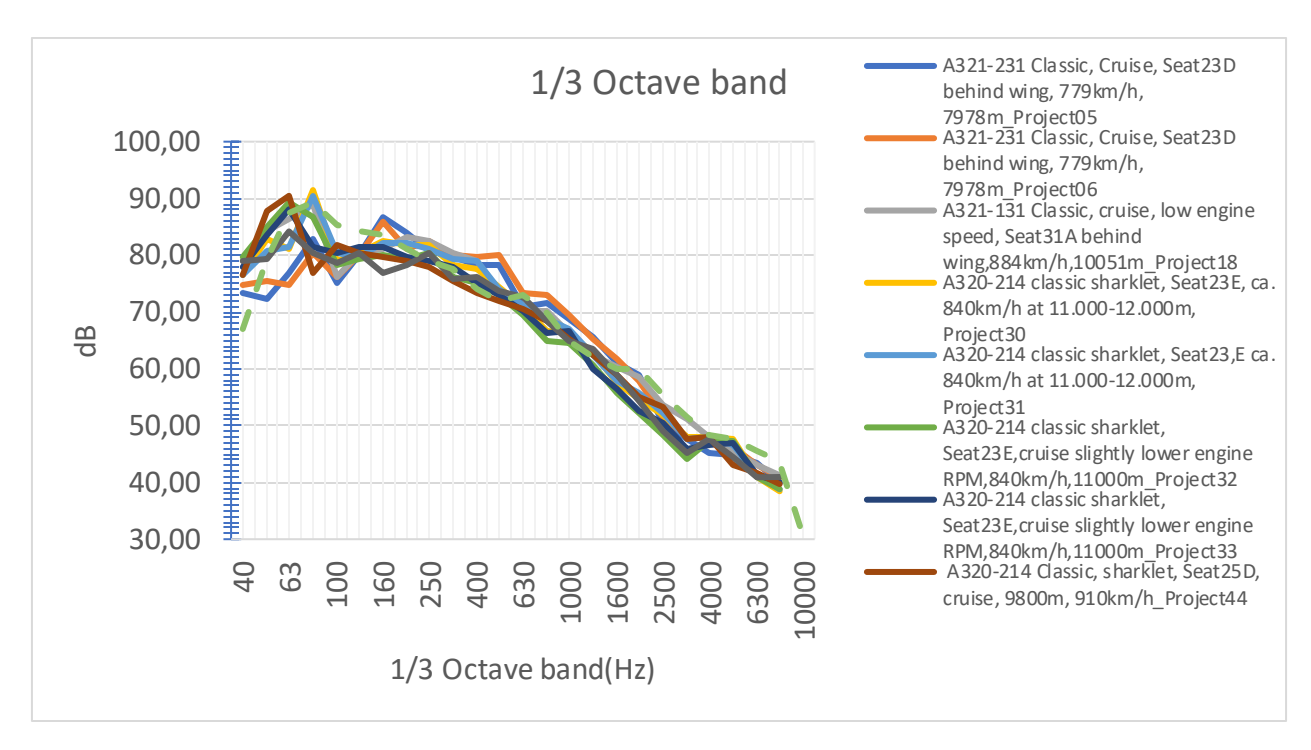


Figure 4: Sound pressure level spectrums considered [dB re 20µPa], Z weighted in third of octave bands.

The setup for the replication in the lab with the A320CEO fuselage section under acoustic excitation has been iteratively improved starting from 3 dodecahedral loudspeakers with 3200W rated electrical power to a final setup that is further used and described. The later excitation consists of two groups of different loudspeakers set aside the fuselage on the two sides.

The overall two-sided excitation consists of the following loudspeakers with their rated electrical power:

- 2x 3000W subwoofer (A)
- 4x 2500W broadband loudspeaker (B)
- 4x 800W dodecahedral mid-high loudspeaker (C)

The setup can be seen in the following Figure 5.

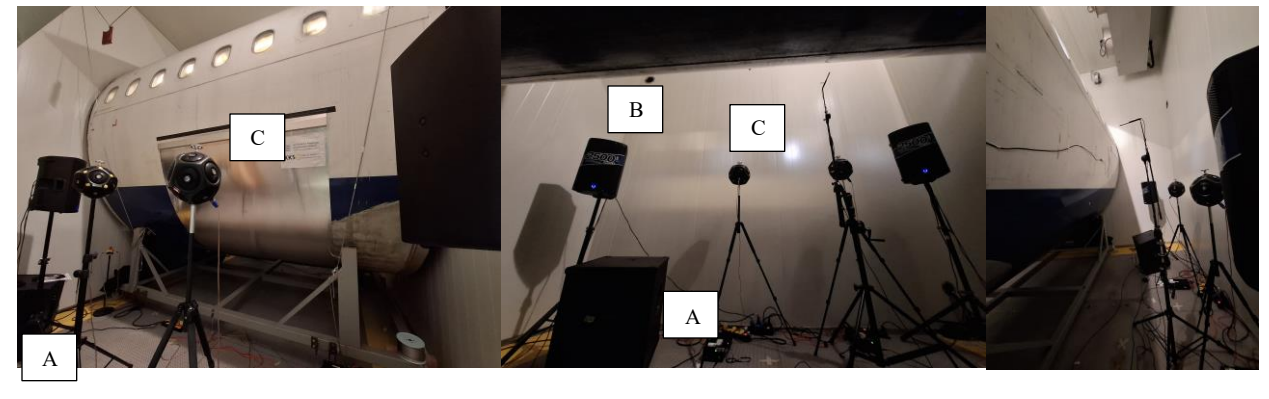


Figure 5: Loudspeaker excitation setup with one subwoofer, two broadband loudspeakers and two dodecahedral on each side of the aircraft fuselage section in the echoic acoustic climate chamber.

The measurements in the lab included different microphone positions on the excitation side in the hall room (chamber) as well as on the response side in the cabin. For some comparison measurements a fixed microphone position was used in the cabin as well as in the hall room. It is understood that local effects, i.e. from room modes may occur on these certain positions. But as the analysis has a clear broadband focus, this is expected to be not of too much importance for i.e. deriving transfer functions.

Obviously, the lab implementation chosen has some limitations to be discussed in section "limitations of the setup". This includes possible structure borne sound paths from loudspeakers through the ground and supporting frame. The first and most simple assumption uses a free-free boundary of the fuselage with only diffuse acoustic excitation. The sound wave field is assumed to be diffuse because of the non-symmetric situated loudspeakers in an oblong box with a large round reflecting surface (fuselage). A wavefield synthesis with phase control over multiple sound sources is not considered here.

These assumptions and simplifications will later be further evaluated.

# RESULTS

The creation of an equivalent acoustic excitation causing the same response spectrum in the cabin as in real flights proved to be more challenging than may be anticipated. In the first place, a professional controller for mechanical environmental testing with random signals was used. The reference microphone in the cabin was used as the control point input to the controller in a response control setup. The drive signal was connected to the loudspeakers. A single axis control was used. However, the equalization of the control parameters proved to be extremely difficult due to many non-linearities in the test setup. A major concern was the automatic and integrated limiting of the loudspeaker amplifiers when some signal properties exceeded certain limits. As a broad band random signal from a vibration controller is only clipping at three times the standard deviation of the drive signal and higher peaks may still occur, the amplifiers were randomly entering their limit mode when tuning the control parameters for each frequency line.

Due to these problems of achieving a stable excitation signal it was then decided to create audio signals offline and "play" them in feedforward to the loudspeakers with the resulting audio spectrum then being measured in the cabin. In a first step the feedforward signal of the excitation was iteratively adjusted to make the response signal match the required measure spectrum from real flights. As only a "reference cruise flight situation" was to be replicated that manual control work was well acceptable and lead to stable and reproducible signals. This process is shown in Figure 6. The later measurements with changed hardware in the loop components and other analysis tasks were performed with the replicated standard excitation as shown in the second step.

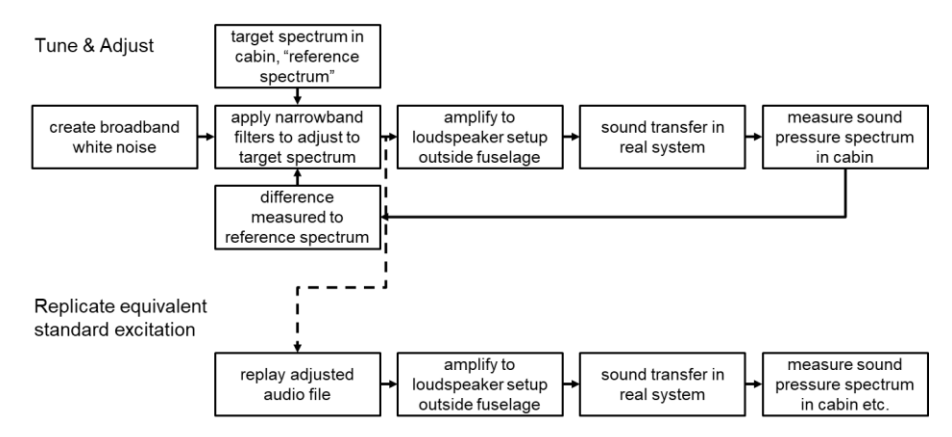


Figure 6: Two-step approach to create an equivalent standard excitation with a first "tune and adjust" step prior to just replicating the created audio file.

#### **EXCITATION AND RESPONSE REALIZED**

With the feedforward implementation a reasonable result was achieved after several iterations by tuning the broad band equalizer bands so that the sound pressure spectrum induced by the outside excitation resembled real flight situations. Figure 7 shows the achieved response sound pressure spectrum in the cabin achieved by the equivalent outside excitation (blue dashed). The figure also shows several sound pressure spectrum measurements from real flights in cruise phase that were chosen a reference signals. The generated response in the test lab was chosen to "smear" a little the tonal peak of the engines' first frequency that is slightly different in each real flight measurement (as the engines' RPMs were). Also, the depiction in thirds of octaves is not favoring a fine resolution of these tonal incidents anyway. The brown dashed curve displays the response by one of the first excitation-tries with only three dodecahedral loudspeakers outside and a datasheet amplifier power supply of 800 W for s comparison of how much the increase of amplifier power enabled a close resemblance of real flight responses in the cabin.

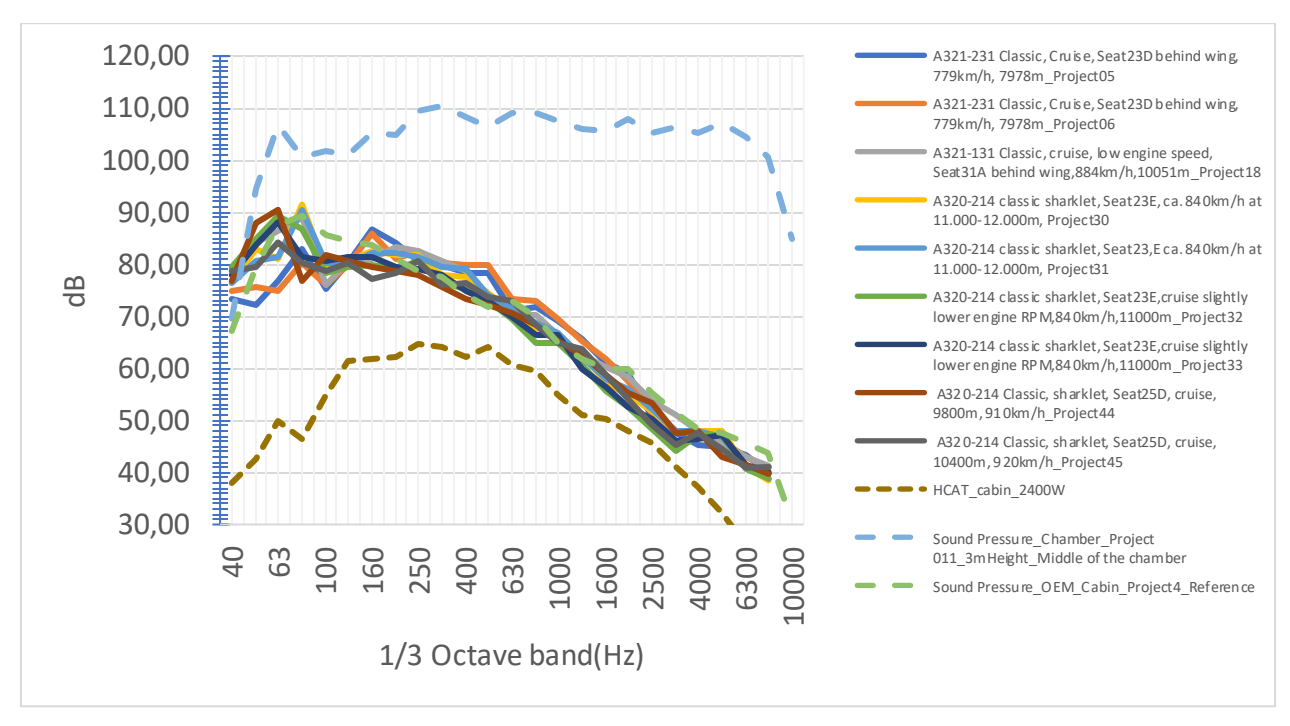


Figure 7: Resulting response in the cabin of the test bed fuselage (green dashed) under equivalent acoustic excitation (light blue dashed) outside. Several selected cruise measurements are display in solid lines.

The overall sound pressure level of the outside spectrum in the reverberation room of the acoustic climate chamber is around 118 dB(Z) re 20  $\mu$ Pa or 117 dB(A) re 20  $\mu$ Pa in Z respectively A weighting.

For more detail, the response (green dashed) to the equivalent excitation (blue dashed) is shown once more with one selected cruise flight (grey solid) in Figure 8.

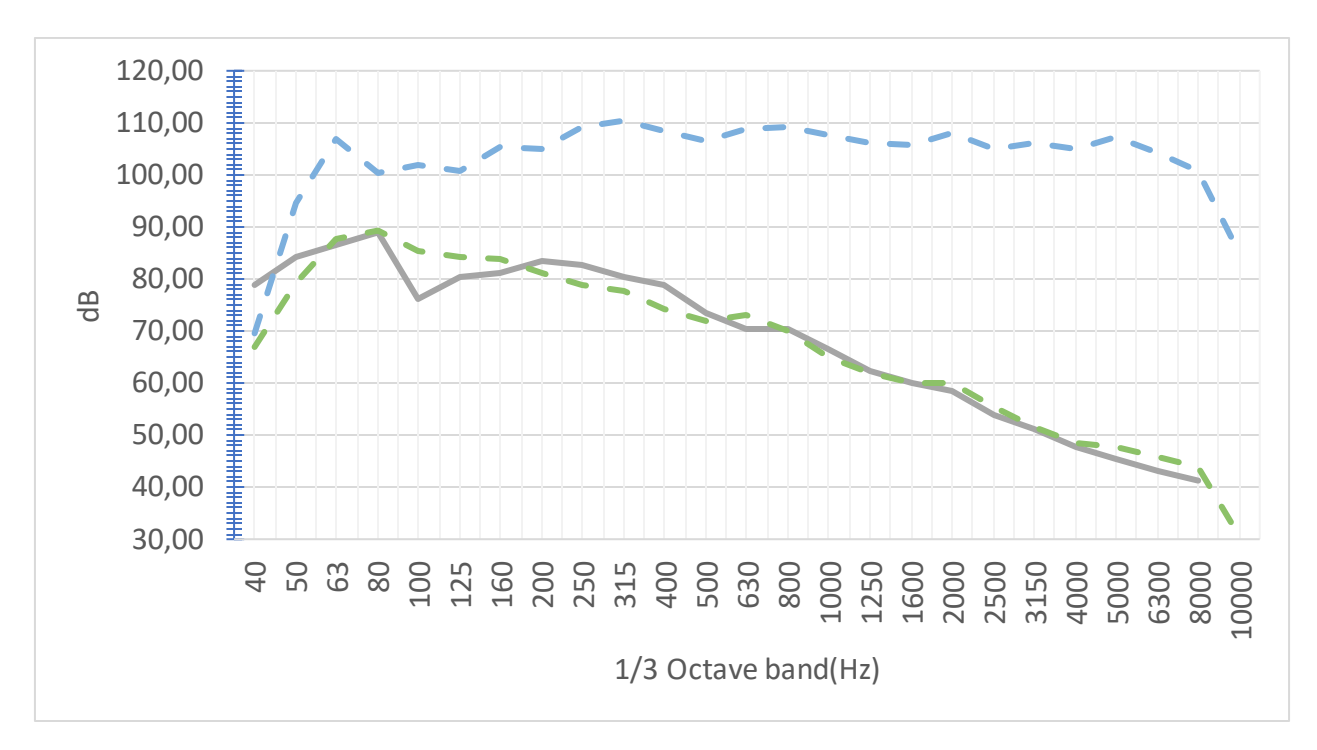


Figure 8: Response (green dashed) and excitation (blue dashed) in more detail.

For looking at the homogeneity of the excitation in the reverberating acoustic climate chamber with the fuselage section in it several sound pressure spectrums were taken at different heights on both sides of the fuselage at different positions from front to aft of the fuselage section. Table 1 shows some LZeq Z-weighted equivalent continuous sound pressure level of the excitation in different positions along the fuselage at different heights.

Table 1: LZeq (dB(Z) re 20 µPa) sound pressure levels at different positions along one side of the fuselage at different heights.

D '.'	TT ' 14	17
Position	Height	LZeq
Backside_right	3,7m	117,36
Backside_right	3,7m	117,32
Backside_middle	3,7m	118,6
Backside_left	3,7m	118,54
Backside_left	3,2m	118,68
Backside_left	3,0m	118,22
Backside_left	2,6m	118,85
Backside_middle	2,6m	119,03
Backside_right	2,6m	118,61
Backside_right	3,0m	118,63
Backside_middle	3,0m	118,4
Backside_middle	3,2m	117,16
Backside_right	3,2m	117,56
Backside_rightmost	3,7m	117,68

For a better visual localization some A-weighted (dB(A) re 20  $\mu$ Pa) sound pressure levels are shown in their rough locations of measurement in Figure 9.

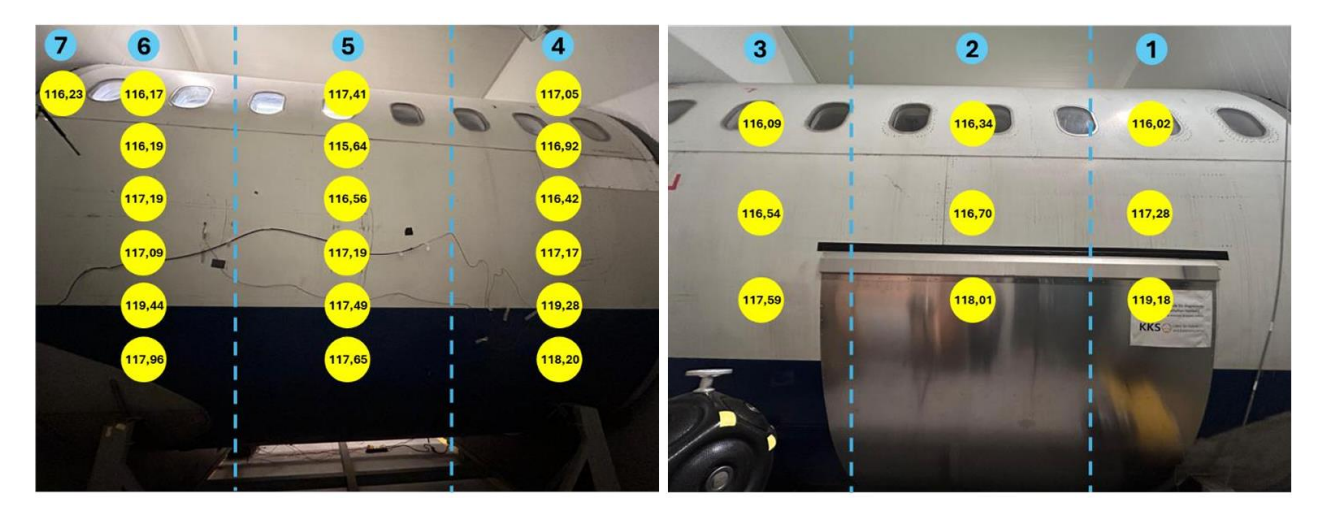


Figure 9: A-weighted sound pressure levels outside of the fuselage in the acoustic climate chamber reverberation room.

It can be concluded that the overall sound pressure level is rather equally exciting the fuselage section in and around the window area and cabin floor area which is the focus of the later studies as shown in [2], [15], [18] and continued in future research.

#### LIMITATIONS OF THE SETUP

Obviously, the current setup has many limitations that need further evaluation and do not allow all possible kinds of analysis performed.

Some deviation from real flight is the necessity to use end cabs at the ends of the fuselage section. Here, foam absorbers and heavy plates are used to shield of unrealistic input at the ends of the fuselage section. The added absorption from 150 mm acoustic foam creates rather low reverberation time in the fuselage section's cabin of around 0.15 s (earlier setups) to 0.2 s in later setups. The last is close to real A320CEO cabins but still slightly too low.

Also, it is obvious that a reverberation chamber for the fuselage section with a length of around 4.5 m will have significant distinctive room modes especially around the lower frequencies especially in the range of the first wavelength and the first harmonics. Depending on the temperature and the actual distance between the different walls, the first static room modes occur at around 60-80 Hz. Higher frequencies of several 100 Hz will however hardly show any global effect as the reflection of the fuselage with the round cross section in the oblong reverberation chamber does create a rather diffuse field with many modes within a small frequency range. However, Finite-Element-Analysis-Simulations (FEA) have shown that the fuselage itself is a comparatively stiff structure compared to the surrounding air and does have a strong effect of special homogenization. Even if some local effects of static room modes cause local differences in excitation sound pressure of the surface area of the fuselage, the effect is smeared well from a few 100 Hz onwards. But it must be noted that the current evaluation is not in any way similar to a correct wavefield replication like in [19], where first blade passing frequencies of open rotor excitations are simulated sweeping of the fuselage.

Another of the limitations is the implemented fixation of the fuselage section. Unlike in real flight, where only the wings exert some lifting power through the center wing box to the connected fuselage sections, the lab setup is resting on a frame that allows for removal from the large acoustic climate chamber. The supporting frame has wheels but rests on wooden blocks like shown in Figure 10 when in test.



Figure 10: Support frame resting on wooden blocks on the floor of the acoustic climate chamber.

The wooden blocks themselves are resting on the floor of the acoustic climate chamber. The frame as well as the metal floor segments have distinctive resonance frequencies that are excited by the broadband random acoustic excitation. It can be noted that some resonances seem to have a significant non-linear behavior because they show very heavily at higher amplitudes while not being significant at lower excitation levels.

The fixation of the fuselage through frame, wooden blocks and metal floor plates forms a structure borne sound path especially for low frequencies excited by the subwoofers standing on the same chamber floor.

To evaluate this effect in a first and rather coarse analysis, low-frequency vibration levels of acceleration in the cabin are compared from real flights to the simulation in the lab with the equivalent acoustic excitation as shown in Figure 11.

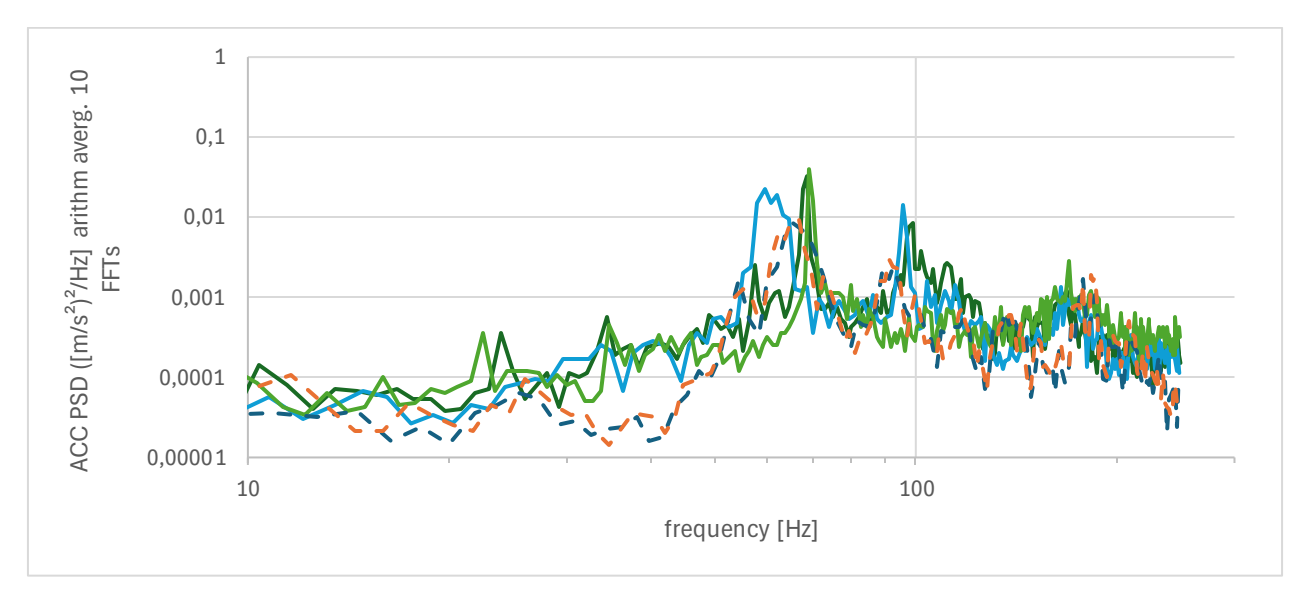


Figure 11: Comparison of vibration acceleration levels measured on the lower mid end of the window sidewall panel in real flight as under equivalent acoustic excitation in the lab.

For this preliminary study only low frequency data was available from measurements with a smartphone at around 500Hz sampling frequency. The same smartphone was used in flight as in lab measurements while being pressed to the lower mid end of the window sidewall panel at the same position. While the values shown may not be accurate on an absolute scale because of the weight of the smartphone and the method of pressing it slightly against the panel, the comparison is still valuable because the same smartphone was used by the same person at the same position. The solid line in Figure 11 show real flight measurement in cruise phase with low engine RPM while the two dashed lines

show the corresponding acceleration spectrums with the same smartphone at the same position in the test lab under equivalent acoustic excitation. First it must be noted that real flight excitations differ significantly. The response in the lab environment falls well within a similar amplitude range. The significant first, second and third order engine rotor dynamics are clearly showing and not aligned to the simulation (which hasn't been tuned to tonal effects). When looked at in thirds of octaves this fine frequency resolution is not seen anyway. The equivalent acoustic excitation could easily be tuned to facilitate different engine RPMs of one certain measurement, but this is not of interest as only broadband frequency effects are studied in the further acoustic analysis.

#### **FURTHER ANALYSIS**

One of the major goals of realizing the test setup with an equivalent acoustic excitation was to study transfer paths from outside to inside. Here, the non-linearity of these transfer paths was of particular interest.

Obviously, low power transfer paths can be studied also by impact or small shaker excitation. But as the structure borne sound paths include many contacts glued or riveted together as well as fasteners like screws or quick connectors, the transfer properties are to be changing significantly when being excited at different levels. This effect is showing when looking at the power transfer from measured sound pressure spectrums outside the fuselage and inside the cabin in Figure 12. Here the Power Spectral Densities of the sound pressure inside the chamber (response) is divided by the sound pressure outside the fuselage (excitation inside the acoustic climate chamber). The transfer functions have been calculated in thirds of octaves for different excitation setups with a rated datasheet power supply of the amplifiers ranging from 2400W to the 19kW in the lasted setup.

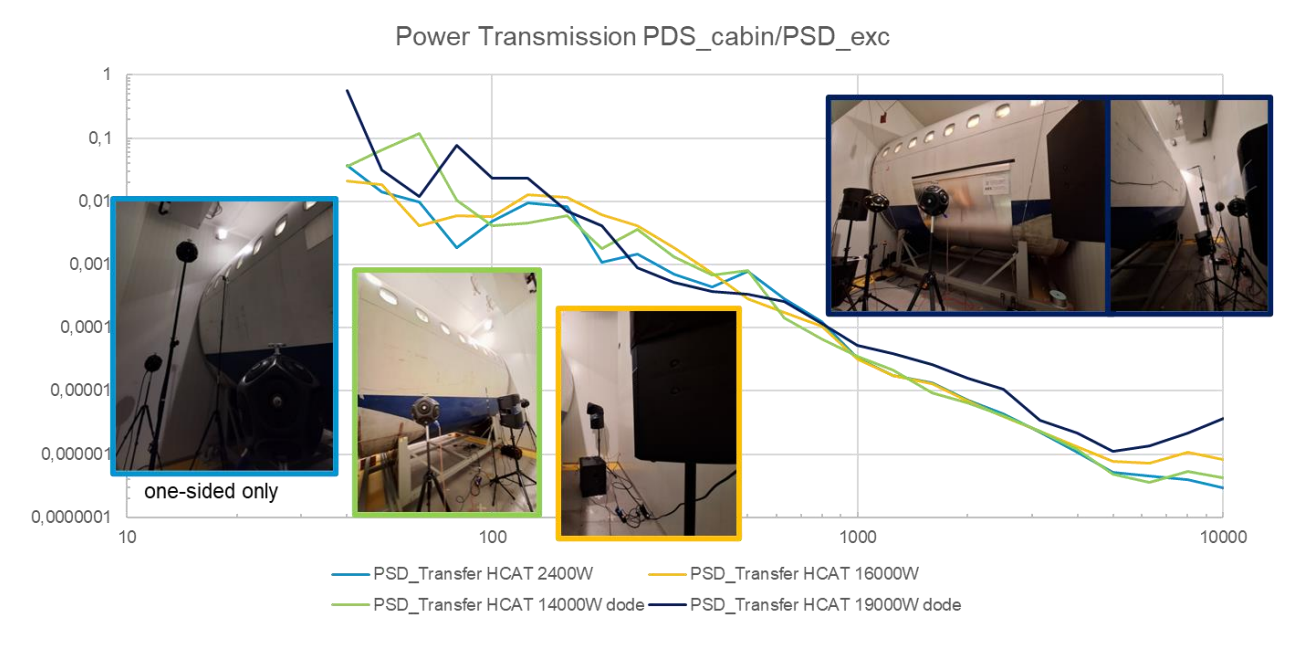


Figure 12: Power transfer functions from outside of the fuselage to the inside in the cabin for different excitation levels.

Even though the excitation levels may be slightly different for the different excitation setups, the transfer functions should exactly the same for a perfect linear system. With deviations of around a decade here and there along the spectrum, a non-linear effect can be found. It is even more of interest that especially the last and most powerful setup created significant deviations from the other less powerful setups. This may originate from non-linearities that occur only at the latest high-power excitations.

Note: The first configuration of 2400 W excitation is on one side of the fuselage only. The diffuse sound field in the reverberation room is however rather similar on both side with only 3-4 dB difference between the side with the loudspeakers and the one without. All other excitation setups have the same excitation on both sides.

### DIFFERENTIATING BETWEEN STRUCTUREBORNE AND ACOUSTICAL TRANSFER

The major goal of creating an equivalent excitation is to measure global sound transfer paths inside the cabin under realistic flight conditions in the lab. As shown in several publications, this approach yielded good and interesting results. More detailed analysis is to come.

One of the more detailed analysis approaches considered here is the differentiation of airborne and structureborne sound power contents within the same sound path.

When sound propagates through the fuselage skin it is - at least for a short time - structureborne only in the skin. After this, different sound paths can be taken to propagate further into the cabin:

- The inside surface of the fuselage skin vibrates and radiates sound, which then could leak through gaps in the inner wall, i.e. gaps between the sidewall panel. This is a purely airborne sound path from the skin onwards
- The sound radiating from the vibrating skin could also excite the inside wall of the doubled-walled-structure causing i.e. the sidewall panel to vibrate and radiate sound to the cabin itself. This is a serial setup of airborne and structureborne transmissions through the double-wall structure.
- The vibrating fuselage skin can also excite other radiating surfaces like the sidewall panel directly through a structureborne transmission through for example brackets that connect the sidewall panel to the fuselage directly. This is a purely structureborne sound path from fuselage skin to the radiating inner surface.

When designing optimized sound reduction treatments considering lightweight design, costs and safety requirements a detailed understanding of the sound paths is necessary. Global sound path tracking [18], i.e. chasing down main sound paths into the cabin with an intensity probe over different surface areas of the inside wall of the cabin is not enough anymore. If, for example, a certain sidewall area radiates a lot of sound power into the cabin, this could have very different roots in the transfer path that require different measures and reduction techniques.

Glass wool, foams or mass layers could be used to reduce airborne sound transmission while structureborne sound paths require methods like isolation with adjusted stiffness, mass and damping properties [15], to name only a few approaches.

Therefore, the ratio of structureborne sound power to airborne sound power within one transfer path is to be studied in more detail.

Here, different approaches can be used. These could include detailed Finite-Element-Models with parameter variations, Frequency-Response-Function (FRF) measurements with force and acceleration measurements or the crosscorrelation analysis presented in the following. The big advantage of the latter one is that only one field quantity like acceleration needs to be measured at different locations unlike full FRF measurements that often need more sophisticated measurement techniques like blocked forces or decoupling to make in-situ measurements under realistic boundary conditions necessary [20], [21], [22], [23].

The following approach will use the equivalent broadband random excitation because it excites the structure with the right power input to minimize amplitude non-linearity issues. Deterministic sine excitation could create transfer functions with less measurement uncertainty but would potentially excite the measured system with nonlinearity effects in amplitude and cross-frequency-coupling messing up the results.

The crosscorrelation gives a time difference between two signals from a convolution calculation of the two signals. Basically, the resulting time difference tau is the average time difference for the most significant similarities (highest in average) between the two signals.

If both signals are very similar with a high coherence, describing the linear relation, then one significant peak in the cross correlation will show the time difference between the two signals. If the two signals are measured acceleration in different positions in a structureborne sound path, then the time difference describes the time the first and significant wave travels through the structure from one point to the other. The magnitude of the peak indicates the convolution of the two signals at that time and will get higher the better the two signals align with that time

difference. High peak magnitudes show that the two signals are very similar under the give time difference of the peak.

When the distance the waves needs to travel through the structure or through air is known, then the speed of sound can be calculated from the measured crosscorrelation time or the first peak. Or vice-versa, if the speed of sound is known (i.e. for air), the distance can be calculates from measured crosscorrelation time of the first peak.

Applied on our analysis task, we can now study, how much of the sound transfer from outside to inside through the double-wall skin/sidewall-system is airborne and how structure borne.

For this, we study the first waves and their time of flight in the crosscorrelation. Later reflections at every connection with changing impedances will create many more peaks in the crosscorrelation plot which cannot be clearly identified anymore. The first peaks can be identified, however with some information we have.

The structureborne sound path from fuselage skin through a bracket into the sidewall panel above the bracket can be geometrically measured. An example is shown in Figure 13. In our case of a A320 classic it is a distance of at least 12,5cm distance between the two walls plus a little extra if the sensors are not perfectly aligned. The exact accelerometer positions on fuselage and window panel should also be considered and may increase that distance a bit. The exact speed of sound is not known because the sound wave will need to travel through parts made of aluminum, rubber, steel and fiber reinforced plastics. It can be assumed to be within a range of 1000m/s to 4000m/s based on the speed of sound of the main material components in that short sound path.

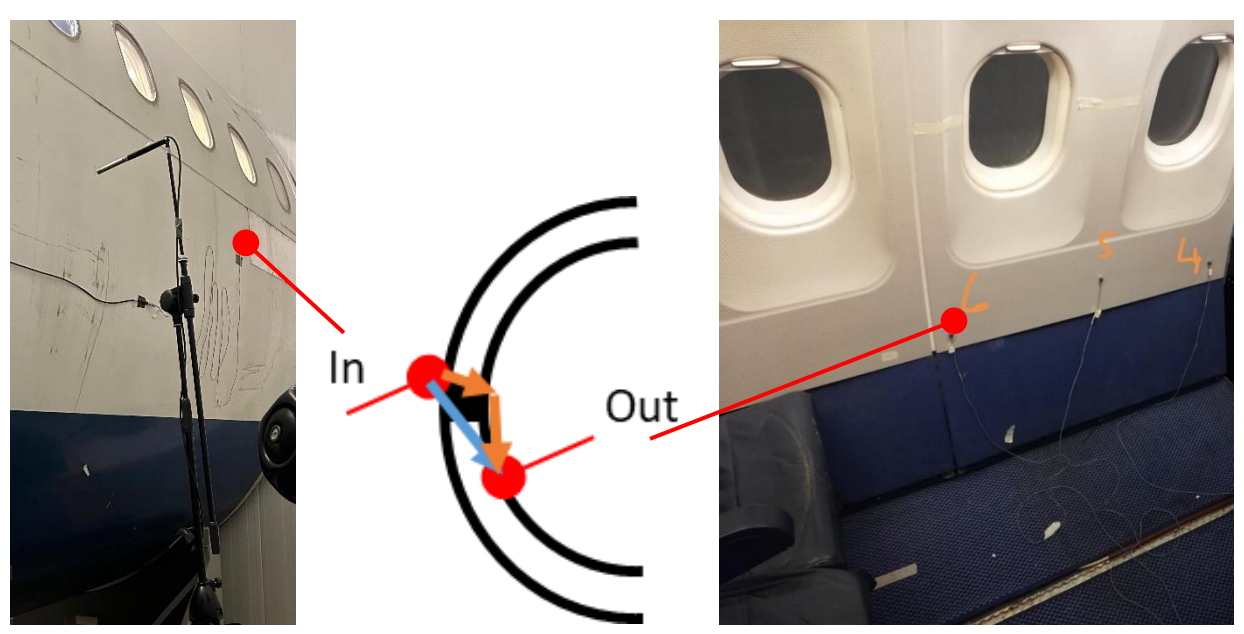


Figure 13: Example studied in the following.

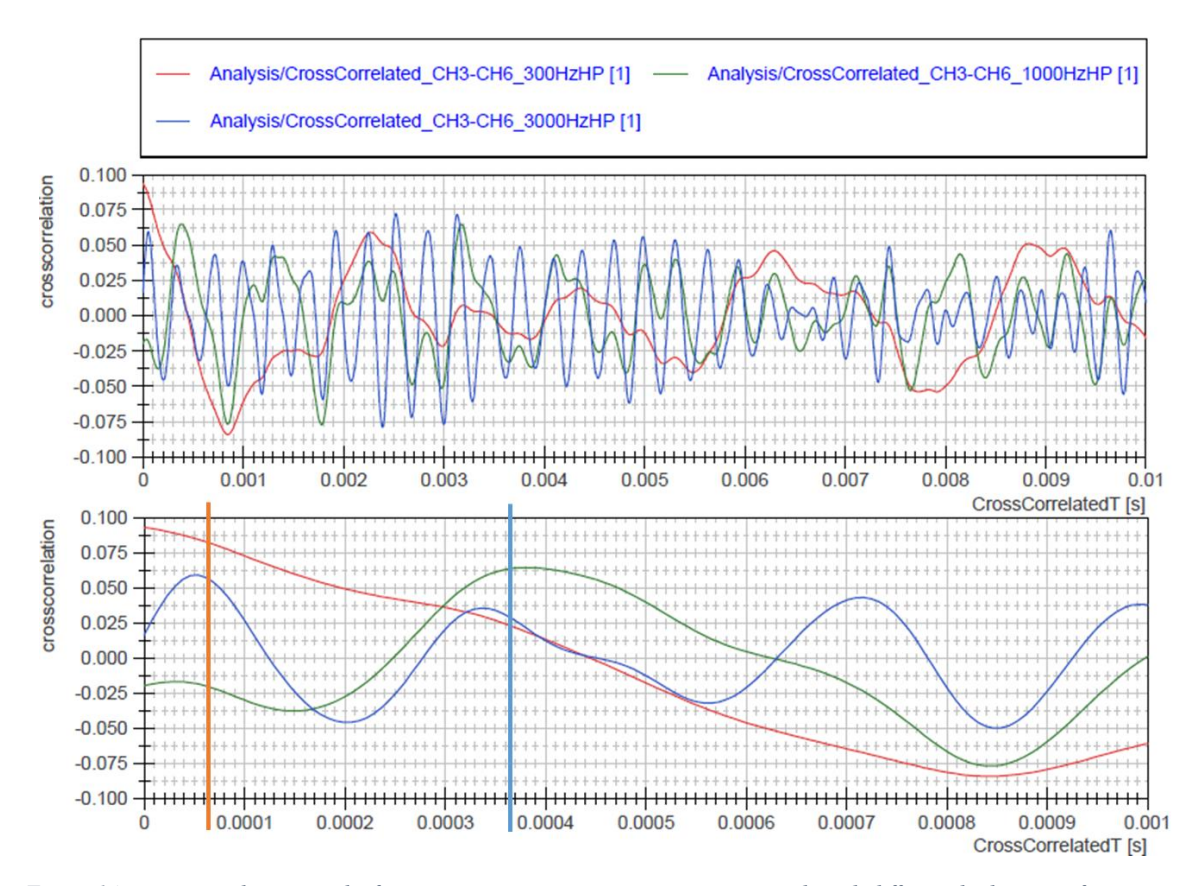


Figure 14: cross correlation results for excitation sensor to response sensor inside with different high passes frequencies.

If we look at Figure 14, we can identify a clear first peak occurring at bit under 0,1 ms, see orange line. When we consider a distance travelled of 125mm, this would lead to an averaged structureborne speed of sound of around 2100 m/s. This seems to be a low speed of sound, but literature shows that this is reasonable for a speed of sound through a series of glass fiber reinforced polymers, elastomers and aluminum.

Contrary to this we look at the airborne contribution on that path, shown with a light blue horizontal line in Figure 14. Here, the distance between the two acceleration sensors was measured to be around 125 mm. The speed of sound under the climatic conditions of the measurement is roughly 340 m/s. This should give a time difference of around 0,36 ms for the distance traveled, see light blue line.

In the plot however, we see this point to be still somewhere on the decaying slope of the structureborne sound path. But we can easily assume that the airborne sound power transfer is significantly lower than the structureborne, at least by the factors given in Table 2.

	frequencies		assumptions			
Correlation amplitude:	>300 Hz	>1000 Hz	>3000 Hz	distance [m]	speed [m/s]	delta t [ms]
airborne amplitude	0,025	0,070	0,035	0,125	340	0,368
structureborne amplitude	0,080	0,020	0,060	0,125	2083	0,060
ratio to airhorne	3.2	0.3	1.7			

Table 2: OEM cabin sidewall panel second from aft in fuselage section, bottom left

If we now take measurements of the sound intensity over the area of interest, in this case measured with a Bruel&Kjaer type 3654/3599 p-p-probe on a type 2270 hand analyzer as shown in Table 3. The measurement area is

a rather small segment bottom left, just above the lining bracket on the window sidewall panel, marked in Figure 13 as "Out".

Table 3: measured sound intensities quadratically averaged from third of octave intensity measurements until 8kHz

measured intensities [W/m²]			
>300 Hz	>1000 Hz	>3000 Hz	area considered [m]
3,04E-06	2,24E-08	7,66E-10	0,01

We then get a power contribution of that reference area under analysis with the following absolute power radiated from that area as in Table 4.

Table 4: calculated power from the considered area for intensities from Table 3 and ration from Table 2.

	power contributions [W]			
	>300 Hz	>1000 Hz	>3000 Hz	
airborne	7,24E-09	1,74E-10	2,82E-12	
structureborne	2,32E-08	4,98E-11	4,84E-12	

These results on the power contribution of airborne and structureborne sound from fuselage skin to a small radiating area above the bracket can be plotted as in Figure 15.

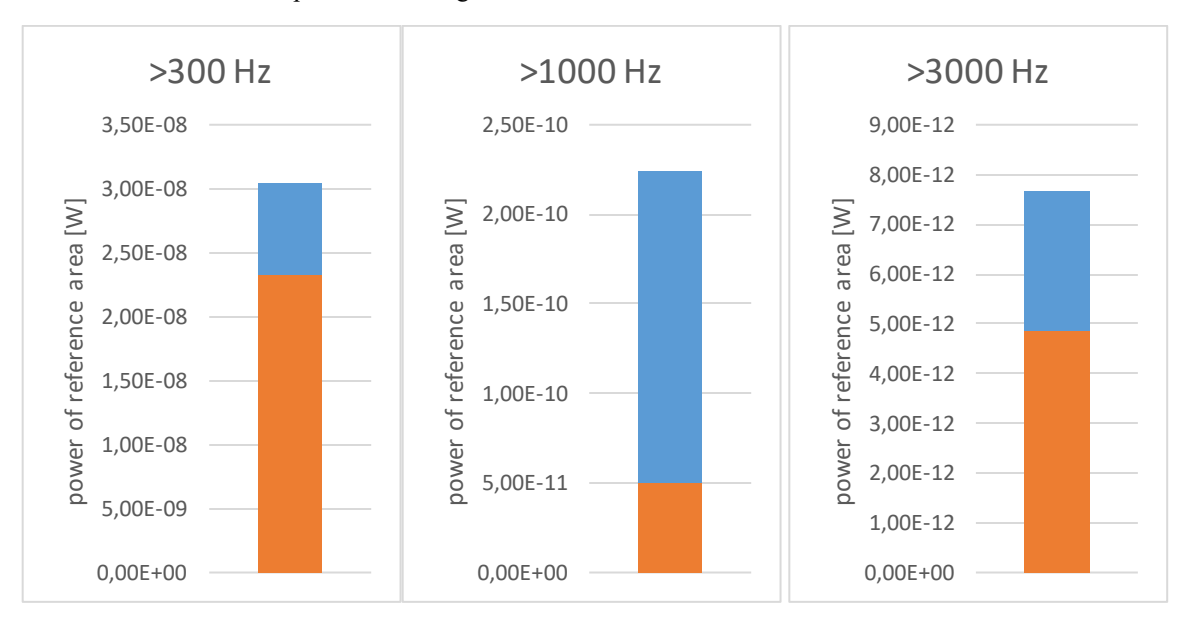


Figure 15: power contributions of radiating surface from structureborne sound path (orange) and airborne (light blue).

It can be noted that the levels of power contribution significantly diminish over several decade for higher high pass cut-off frequencies as would be expected from the green dashed curve in Figure 8 for the cabin sound spectrum.

Furthermore, it can be seen that the structureborne sound path is more relevant that the airborne in lower and higher frequency bands but not around 1000 Hz. This may result from increasing sound reduction on the airborne sound path above 1000 Hz and decoupling or isolation effects working on frequencies above the 300 Hz threshold.

# **CONCLUSIONS**

The paper describes the setup of an acoustic excitation tests with a reverberation room in an acoustic climate chamber that excites an A320CEO fuselage section in such a way that the sound pressure spectrum inside the fuselage section matches measurements from real flights in cruise phase of A320-CEO-family aircraft.

The setup described and measured uses different loudspeaker systems creating a near-diffuse sound field outside the fuselage. The measured response inside the cabin is matching not only in overall sound pressure spectrum the real flights but also surface vibrations on the sidewall panel is within typical vibration spectrum ranges of real flights.

It also describes limitation of the setup chosen and how they are treated in some analysis approaches presented. One of the applications presented is the detailed in-situ measured of sound transfer paths under realistic sound power excitations. This also includes an analysis focusing on crosscorrelation analysis to study the ratio of structureborne to airborne transfer power.

The setup will be used for more in-depth analysis of transfer paths under various cabin setups and noise reduction treatments in the near future. With the developed setup, in-situ studies of various developments can be studied to find optimum solutions under several design goals like noise reduction, lightweight design and cost-saving. Especially, mass-intensive treatments should be replaced by better or equally performing lighter treatments. This is deemed to be of significance especially with much louder future propulsion systems now under consideration for higher fuel efficiency like open rotor designs, ultra-high-bypass-ration engines and any kind of electrically actuated propeller propulsion.

#### **AUTHOR STATEMENTS**

The LuFo VI-2 research project "ENTIRETY" is kindly funded by the German ministry of economic affairs and climate action "BMWK". The presentation at SAVE was funded by the Research and Transfer Center Future Air Mobility by the Hamburg University of Applied Sciences (HAW Hamburg).

# REFERENCES

- [1] U. Orrenius, V. Cotoni, and A. Wareing, "Analysis of sound transmission through aircraft fuselages excited by turbulent boundary layer or diffuse acoustic pressure fields," 38th International Congress and Exposition on Noise Control Engineering 2009, INTER-NOISE 2009, vol. 4, pp. 2637–2645, Jan. 2009.
- [2] B. Plaumann, T. Ziegner, T. Tews, and J. Hansen, "Untersuchung und Optimierung der Schallpfade in die VIP-Kabine," Tagungsband Proceedings "Fortschritte der Akustik DAGA 2023": DAGA 2023: 49. Jahrestagung für Akustik, 06.-09. März 2023 in Hamburg, 2023, doi: 10.48441/4427.720.
- [3] A. Chodvadiya, B. Plaumann, E. Hein, T. Tews, J. Hansen, and P. Cordes, "Influence of VIP floor setups on noise reduction in aircraft cabin," *Tagungsband Proceedings "Fortschritte der Akustik DAGA 2024"*: DAGA 2024 50. Jahrestagung für Akustik, 18. 21. März 2024, Hannover, pp. 592–595, 2024, doi: 10.48441/4427.1502.
- [4] K. Ozcan and S. Nemlioglu, "In-cabin noise levels during commercial aircraft flights," *Canadian Acoustics Acoustique Canadienne*, vol. 34, Dec. 2006.
- [5] H. P. Lee, S. Kumar, S. Garg, and K. M. Lim, "Assessment of in-cabin noise of wide-body aircrafts," *Appl Acoust*, vol. 194, p. 108809, Jan. 2022, doi: 10.1016/j.apacoust.2022.108809.
- [6] N. Hu, H. Buchholz, M. Herr, C. Spehr, and S. Haxter, "Contributions of Different Aeroacoustic Sources to Aircraft Cabin Noise," in *19th AIAA/CEAS Aeroacoustics Conference*, Reston, Virginia: American Institute of Aeronautics and Astronautics, 2013. doi: 10.2514/6.2013-2030.
- [7] C. Thomas and H. Scheel, "Kabinenakustik in der Luftfahrtforschung," p. 7 pages, 2019, doi: 10.25967/480290.
- [8] J. Yang, M. Wu, and L. Han, "A Review of Sound Field Control," *Applied Sciences*, vol. 12, no. 14, p. 7319, Jan. 2022, doi: 10.3390/app12147319.

- [9] L. Liu, Y. Yu, Y. Qiu, X. Zheng, Z. Dai, and Y. Cui, "Reproduction of sound field inside an aircraft mock-up for evaluating ANC devices," *Applied Acoustics*, vol. 188, p. 108588, Jan. 2022, doi: 10.1016/j.apacoust.2021.108588.
- [10] P.-A. Gauthier, C. Camier, F.-A. Lebel, Y. Pasco, and A. Berry, *Experiments of sound field reproduction inside aircraft cabin mock-up*, vol. 2. 2012.
- [11] P.-A. Gauthier, C. Camier, O. Gauthier, Y. Pasco, and A. Berry, "Sound field reproduction of real flight recordings in cabin mock-up," in *Audio Engineering Society Conference: 52nd International Conference: Sound Field Control-Engineering and Perception*, Audio Engineering Society, 2013.
- [12] P.-A. Gauthier *et al.*, "Experiments of multichannel least-square methods for sound field reproduction inside aircraft mock-up: Objective evaluations," *Journal of Sound and Vibration*, vol. 376, pp. 194–216, Aug. 2016, doi: 10.1016/j.jsv.2016.04.027.
- [13] Gh. R. Sinambari and S. Sentpali, *Ingenieurakustik*. Wiesbaden: Springer Fachmedien Wiesbaden, 2020. doi: 10.1007/978-3-658-27289-0.
- [14] P. Cordes, Y. Hoven, P. Joshi, B. Plaumann, T. Tews, and J. Hansen, "Validierung eines virtualSEA Modells eines Flugzeugseitenwandausschnitts," in *Fortschritte der Akustik*, Deutsche Gesellschaft für Akustik e.V., 2024, pp. 612–615. Accessed: Jan. 07, 2025. [Online]. Available: https://reposit.haw-hamburg.de/handle/20.500.12738/15812
- [15] E. Hein, A. Chodvadiya, B. Plaumann, and T. Tews, "Reduktion von Schallleistungsbeiträgen in der Flugzeugakustik durch individuell ausgelegte Isolatoren," presented at the Deutscher Luft- und Raumfahrtkongress 2024, Deutsche Gesellschaft für Luft- und Raumfahrt Lilienthal-Oberth e.V., Nov. 2024. doi: 10.25967/630130.
- [16] "Easy Access Rules for Large Aeroplanes (CS-25) Revision from June 2022 Available in pdf, online & XML format: All files (pdf, online format, xml) were replaced on 30 January 2023. The corrections are described in the notes underneath individual files. | EASA." Accessed: Jan. 14, 2025. [Online]. Available: https://www.easa.europa.eu/en/document-library/easy-access-rules/easy-access-rules-large-aeroplanes-cs-25
- [17] W. Kleppmann, *Versuchsplanung: Produkte und Prozesse optimieren*, 10., Überarbeitete Auflage. in Praxisreihe Qualität. München: Carl Hanser Verlag GmbH & Co. KG, 2020.
- [18] T. Ziegner, "Quantifizierung und Modellierung von Schallleistungsbeiträgen in der VIP Flugzeugkabine," Nov. 2024, doi: 10.25967/630539.
- [19] M. Wandel, C. Thomas, and M. Teschner, "Acoustic Flight-Lab-Eine einzigartige Integrationsplattform zur Optimierung vibro-akustischer Maßnahmen an Flugzeugen, 49," *Jahrestagung für Akustik (DAGA)*, 2023, Accessed: Jan. 14, 2025. [Online]. Available: https://pub.dega-akustik.de/DAGA 2023/data/articles/000129.pdf
- [20] D. Klerk, D. J. Rixen, and S. N. Voormeeren, "General Framework for Dynamic Substructuring: History, Review and Classification of Techniques," *AIAA Journal*, vol. 46, no. 5, pp. 1169–1181, Jan. 2008, doi: 10.2514/1.33274.
- [21] M. V. van der Seijs, D. de Klerk, and D. J. Rixen, "General framework for transfer path analysis: History, theory and classification of techniques," *Mechanical Systems and Signal Processing*, vol. 68–69, pp. 217–244, Feb. 2016, doi: 10.1016/j.ymssp.2015.08.004.
- [22] M. S. Allen, R. L. Mayes, and E. J. Bergman, "Experimental modal substructuring to couple and uncouple substructures with flexible fixtures and multi-point connections," *Journal of Sound and Vibration*, vol. 329, no. 23, pp. 4891–4906, Nov. 2010, doi: 10.1016/j.jsv.2010.06.007.
- [23] S. N. Voormeeren and D. J. Rixen, "A family of substructure decoupling techniques based on a dual assembly approach," *Mechanical Systems and Signal Processing*, vol. 27, pp. 379–396, Feb. 2012, doi: 10.1016/j.ymssp.2011.07.028.